



# Development of *In Silico* Analysis and Molecular Dynamics Simulation on L67P and D76Y Mutants of the Human Superoxide Dismutase 1(hSOD1) Related to Amyotrophic Lateral Sclerosis

Payam Baziyar<sup>1</sup>, Bagher Seyedalipour<sup>1\*</sup>, Saman Hosseinkhani<sup>2</sup>, Ehsan Nazifi<sup>3</sup>

<sup>1</sup> Department of Molecular and Cell Biology, Faculty of Basic Science, University of Mazandaran, Babolsar, Iran.

<sup>2</sup> Department of Biochemistry, Faculty of Biological Sciences, Tarbiat Modares University, Tehran, Iran.

<sup>3</sup> Department of Biology, Faculty of Basic Science, University of Mazandaran, Babolsar, Iran.

\*Corresponding author: Bagher seyedalipour, Department of Molecular and Cell Biology, Faculty of Basic Science, University of Mazandaran, Babolsar, Iran. Tel/Fax: +98-1135302405, E-mail: [b.seyedalipour@umz.ac.ir](mailto:b.seyedalipour@umz.ac.ir)

**Background** One neurodegenerative disorder that is caused by a mutation in the hSOD1 gene is Amyotrophic lateral sclerosis (ALS).

**Objectives:** The current study was developed in order to evaluate the effect exerted by two ALS-associated point mutations, L67P and D76Y are located in the metal-binding loop, on structural characterization of hSOD1 protein using molecular dynamics (MD) simulations and computational predictions.

**Materials and Methods:** In this study, GROMACS was utilized to perform molecular dynamics simulations along with 9 different algorithms such as Predict SNP, PhD-SNP, MAPP, PolyPhen-1, Polyphen-2, SNP, SIFT, SNP&GO, and PMUT for predicting and also evaluating the mutational effect on the structural and conformational characterization of hSOD1.

**Results:** Our study was done by several programs predicting the destabilizing and harmful effect exerted by mutant hSOD1. The deleterious effect of L67P mutation was predicted by MAPP and PhD-SNP algorithms, and D76Y mutation was predicted by 9 algorithms. Comparative studies that were conducted on mutants and wild-type indicated the alteration in flexibility and protein conformational stability influenced the metal-binding loop's conformation. The outcomes of the MD exhibited an increase and decrease of flexibility for D76Y and L67P mutants compared to the wild type, respectively. On the other hand, analysis of the gyration radius indicated lower and higher compactness for D76Y and L67P, respectively, suggesting that replacing amino acid at the metal-binding loop can alter the protein compactness compared with the protein the wild type.

**Conclusions:** Overall, these findings provided insight into the effect of mutations on the hSOD1, which leads to neurodegeneration disorders in humans. The results show that the mutations of L67P and D76Y influence the stability of protein conformational and flexibility associated with ALS disease. Thus, results of such mutations are can be a prerequisite to achieve a thorough understanding of ALS pathogenicity.

**Keywords:** Amyotrophic lateral sclerosis (ALS), D76Y and L67P variants, Human superoxide dismutase-1 (hSOD1), Metal-binding loop (MBL), Molecular dynamics (MD) Simulation

## 1. Background

One neurodegenerative disease caused by a single gene mutation is known as Amyotrophic lateral sclerosis (ALS) that is also known as Lou Gehrig's disease (1, 2).

The disease affects both the upper and the lower motor neurons and leads to muscular paralysis (3). Depending on the family history of the disease or its absence, ALS occurs in sporadic and familial forms. About 10

percent of ALS is familial, caused by mutations that are genetic, that is passed on by a family member (2). About 90% of ALS cases are sporadic ALS, probably due to environmental and genetic risk factors. Among the known genes related to ALS, hSOD1 (Human Cu/Zn Superoxide Dismutase) gene is still a significant causing fALS and this gene has been studied widely. The hSOD1 was the first mutated gene linked to fALS, and the ALS genetic form was mostly passed on and linked to 21q22.11, in which the hSOD1 gene is located (4-6). The hSOD1 is an important antioxidant defense enzyme at the forefront of superoxide disintegration in nearly all living cells (7). The hSOD1 is a 153 amino acid protein in each subunit (16 kDa), forming 32 kDa (8). Each hSOD1 monomer consists of zinc, copper, and two metal ions, and they have a catalytic and structural role in the enzyme. Zinc has some dual role in keeping the catalytic activity and structural integrity of hSOD1. Each monomer consists of an and electrostatic loop and some metal bonding loop (loop IV, 50-83) (loop VII, residues 121–142) (9). The copper ion is bound to four histidine's 46, 48, 63, and 120, and Zinc ion is bound to three histidine's 63, 71, 80, and aspartate 83 that are in the zinc loop are linked by an intra-subunit disulfide bridge to the  $\beta$ -barrel (10). The Copper and zinc coordinating sites are linked by His63 and, along with the three other histidine residues, maintain the very copper that is in a distorted square planar geometry. The copper ion operates as a redox partner for and it is solvent-exposed. In contrast, interestingly the zinc ion is completely embedded in the  $\beta$ -barrel and it is crucial to stabilize its structure. Thus, both intersubunit disulfide bonds and Cu/Zn metalation are considered to be important to keep hSOD1 structural integrity (4, 11, 12). Some new missense was reported by Grande *et al.* for the first time (203T >C) in exon 3 of the hSOD1 gene, which causes leucine to be replaced by proline (L67P) (13). Krieger *et al.* made the second report concerning missense mutation in 203T > C exon 3 of the hSOD1 gene in an ALS patient (14). The D76Y is another missense mutation (230 G>T) that also occurs in exon 3. The D76Y mutation was previously reported in a Danish family and was found in sporadic and familial ALS cases in England and New Zealand (15). The Zn-subloop contains D76 and it is a highly preserved residue in various organisms. More than 60% of hSOD1 mutations are found at exons 4 and 5. Though there is only a limited number of mutations reported in exon 3.

In ALS patients, the missense substitutions that are at surface residues D76, N86, D90, D101, and N139 have been detected thus far. It was predicted that a subset of some known substitutions at these residues, like D76Y, and D101N diminish critical hydrogen salt bridges or bonds between the residues in some different elements of the very protein (16-19). Leucine 67 supports the salt bridge between arginine 69 and glutamate 77 at the Zinc binding region, but at the outside edge of the stack, the region precludes an electrostatic interaction. One of the features that is vital to the membrane-anchoring role of Zn-binding loop is the proximity of the hydrophobic Leu67 side chain and positively charged Arg69 side chain (20, 21). ALS-associated hSOD1 may affect protein structure and properties, leading to protein folding and dysfunction, as previously reported *in vitro*. (22).

On the other hand, mutations reported in exon regions of the hSOD1 gene showed that their toxic effects result from protein dysfunction with increased oxidative stress (23). Previously, more than 120 single nucleotide variants (SNVs) related to ALS have been described for hSOD1. All fALS-hSOD1 mutations cause almost the same disease, and result, the rate of disease progression varies significantly between mutations (24, 25). The biophysical properties of the protein can be affected by the mutations that occurred in a long distance from the active site and the mutations near the metal-binding site, which eventually results in protein aggregation and misfolding (26, 27). The accumulation tendency in mentioned mutant proteins can assist other researchers with anticipating their aggregations in the laboratory. Despite the laboratory methods, computer simulations can assess procedures at the atomic and molecular levels quickly and at a lower cost and obtain valuable information about optimizing experimental operations (28). Computer simulations, commonly referred to as *in silico* analysis, became an effective method in studying disease-causing mutations and their effects on the structure of proteins. Therefore, computational tools have become essential as an experimental method for studying SNVs (29).

## 2. Objectives

This study focused on the possible effects of L67P and D76Y mutations in the metal-binding loop on parameters that are structural like flexibility and stability, and also their comparison with the wild-type by molecular

dynamics simulation. Zn ion is very significant to maintain the structure of hSOD1, and its loss disrupts loop function (loop IV). The important is that Zn has a lower affinity to hSOD1 than Cu, implying that hSOD1 may be more prone to losing Zn ions. Removing Zn ions in hSOD1 can cause ALS through altering the pattern of protein folding and affecting catalytic activity (30,31). Thus, molecular dynamics simulation has been widely utilized in studying the stability of protein, conformational change. Molecular dynamics simulation aims to calculate the trajectories of proteins and examine their actual behavior over time. The exact information on protein conformational fluctuations and changes can be applied to assess some structural parameters like flexibility and stability during this process (32,33). This study discusses the dynamic features of these mutants and their connection with protein aggregation at the molecular level. The results and discoveries of this study might be helpful as a diagnostic and/or predictive instrument to analyze the impact of mutations by connecting the critical stages of disease development to changes in the stability of hSOD1. These changes may negatively affect hSOD1 and illustrate their association with FALS. Comprehension of the effects exerted by hSOD1 mutations on the structure of protein and function can shed light on the design of further experiments and provide relevant information on the molecular mechanism of FALS.

### 3. Materials and Methods

#### 3.1. Structure Data and Sequence

The sequence of hSOD1 sequence ID: P00441 that was extracted from the UniProt Knowledgebase (9). Retrieval and geometry optimization native hSOD1 structure was gained from PDB (PDB ID: 2C9V) at the high resolution of 1.07 Å, and mutations were performed in UniProt Knowledgebase (UniProtKB) (34,35).

#### 3.2. SNP Analysis

In fact, the most common genetic variation found in the human genome is the Single nucleotide polymorphisms (SNPs) are. There are many computational algorithms that are used in predicting the effects exerted by of amino acid substitution on the function the structure of protein. These different algorithms are in fact designed with the aim of predicting if a particular substitution

proves to be deleterious or neutral according to some different parameters obtained from the structural, Physico-chemical, or evolutionary characteristics. (36-39). The effects of mutations (L67P and D76Y) on the function of hSOD1 protein were analyzed by Predict SNP integrated server (<https://loschmidt.chemi.muni.cz/predictsnp/>). PREDICT SNP is a consensus classification that combines the 9 algorithms (Predict SNP, MAPP, PolyPhen-1, Polyphen-2, SIFT, SNP&GO, PMUT, SNAP, and PhD-SNP), for precise prediction together with predictive score (40). Interestingly, we carried out an *in silico* analysis through six stability predictor algorithms ( I-mutant2 PDB, AUTO-MUTE SVM, AUTO-MUTE RF, DUET, mCSM, and ENCoM) on hSOD1(35). Thus, we collected the WT-hSOD1 and mutants of hSOD1 as for *in silico* analysis, that is able to determine if the mentioned variants affect the stability of protein of its three-dimensional structure.

#### 3.3. Molecular Dynamics

The mutants (L67P and D76Y) and hSOD1 wild type (PDB ID: 2C9V) Using the GROMACS Package version 5.1 and Pymol software (<http://www.pymol.org>), were generated on the 2C9V file (41). Each molecular simulation lasted for 50000 ps at 1 fs per step. The MD trajectories were analyzed using parameters: root-mean-square fluctuation (RMSF), hydrogen bonds (H-bond), root-mean-square deviation (RMSD), and the radius of gyration (Rg) (42-44). The MD simulations for hSOD1 mutants and wild-type with force field GROMOS9643 a1 and SPC216 as the water was applied so as to solvate the structures that is in a cubic box. The addition of ions to make the simulation system that is electrically neutral was done through adding two sodium ions and one sodium ion for the D76Y and L67P mutations, respectively. After minimization, three steps were conducted in the MD simulation. The NVT (volume, temperature, and constant number), and also NPT (temperature, constant number, pressure) ensemble was carried out at 298 K and 1 atm for 2000 ps. In fact, the MD simulations were conducted at 298 K and pH=7.4 for 50 ns for the hSOD1 mutants and wild-type.

#### 3.4. Evaluation of Structural and Conformational Changes in the Mutated Protein

One program for the analysis of molecular structures, the interactive visualization and related data is UCSF

Chimera (<https://www.cgl.ucsf.edu/chimera/download.html>) which provides the access to numerous settings of parameters via graphical interfaces. Chimera (version 1.12) was used to generate the mutated 3D model of each human SOD1 protein. The (PDB ID: 2C9V) was obtained in National Center for Biotechnology Information (NCBI). The sequence in the chain was presented, the region of mutations was selected and colored. The structural model of the protein was obtained.

## 4. Results

### 4.1. Analysis of SNP

The analysis of the impact exerted by mutations on hSOD1 protein was performed by 9 algorithms, PMUT, SNP&GO, SIFT, SNP, MAPP, PolyPhen-1, PolyPhen-2 of Predict SNP, PhD-SNP (**Table 1**). The results of PREDICT-SNP analysis for the D76Y mutation showed that 9 algorithms evaluated this mutation as destructive. In contrast, the L67P mutation was predicted as deleterious by 4 algorithms and was predicted as neutral by 5 algorithms. The impact exerted by the mutations on hSOD1 stability and structure was further evaluated using  $\Delta\Delta G$  calculation with web servers including

I-mutant2 PDB, AUTO-MUTE SVM, AUTO-MUTE RF, DUET, mCSM and ENCoM (**Table 2**). The results of protein stability analysis for the L67P and D76Y mutations exhibit destabilizing effects on the stability of the WT-hSOD1 structure. The use of multiple algorithms provides greater reliability.

### 4.2. Evaluation of Structural and Conformational Changes in the Mutated Protein

Using Chimera software version 1.12 (PDB ID: 2C9V), the general schematic of hSOD1 and the location of the investigated mutants (L67P and D76Y) are indicated in **Figure 1A**. We have observed alterations in the interaction of adjacent amino acids and structural alterations in wild-type and mutants L67P and D76Y (**Fig. 1B-G**). The results showed that the size of amino acids changed compared to the wild type.. For L67P and D76Y, the two probabilities of simultaneous rotation with the probability coefficient were examined, respectively. These alterations can affect protein conformation and thus lead to misfolding. In other words, it can be said that these mutations could be related to the possible accumulation of hSOD1 and, consequently ALS.

**Table 1.** Functional prediction of hSOD1 variants by nine SNP prediction algorithms

	L67P		D76Y
Predict SNP	Neutral	Predict SNP	Deleterious
MAPP	Deleterious	MAPP	Deleterious
PhD-SNP	Deleterious	PhD-SNP	Deleterious
PolyPhen-1	Neutral	PolyPhen-1	Deleterious
Polyphen-2	Neutral	Polyphen-2	Deleterious
SIFT	Neutral	SIFT	Deleterious
SNP&GO	Deleterious	SNP&GO	Deleterious
PMUT	Deleterious	PMUT	Deleterious
SNAP	Neutral	SNAP	Deleterious

The SNP prediction were performed pH=7.4 at 25 °C for the hSOD1 wild-type (PDB ID: 2C9V) and mutants (L67P and D76Y). Abbreviations: SNP, single-nucleotide polymorphism; hSOD1, human superoxide dismutase-1.

**Table 2.** Performance effect of mutation on protein stability *in silico* analysis of hSOD1 mutants

Programs	D76Y	L67P	Results
	$\Delta\Delta G$ (Kcal.mol <sup>-1</sup> )	$\Delta\Delta G$ (Kcal.mol <sup>-1</sup> )	
I-mutant2.0 PDB	-0.32	-0.96	Decreases
AUTO-MUTE SVM	-0.1	-1.17	Decreases
AUTO-MUTE RF	-1.65	-1.38	Decreases
DUET	-0.181	-0.529	Destabilizing
mCSM	-0.22	-0.180	Destabilizing
ENCoM	-0.215	-0.428	Destabilizing

The protein stability was performed pH=7.4 at 25 °C for the hSOD1 wild-type (PDB ID: 2C9V) and mutants (L67P and D76Y).

#### 4.3. Molecular Dynamics

In fact, as asserted in the materials and methods section, the simulation by molecular dynamics (MD) is done through using the GROMACS Software were performed. In addition, MD trajectories of hSOD1 WT and L67P and D76Y as its variants were applied to make a backbone RMSD plot. The calculation of root-mean-square deviation (RMSD) was made by the total number of conformations that were made over a 50 ns simulation (**Fig. 2**). The results of RMSD both L67P and D76Y variants exhibit an initial increase and up to 29 nm a stable and convergent structure. Then, a sudden rise in RMSD values was seen between 30 and 35 ns for the D76Y variant. After 35 ns, all relevant structures seem to float a stable conformation. The RMSF values show that the D76Y mutant has some greater fluctuations compared to the L67P mutant and wild-type (**Fig. 3**). In wild-type and L67P mutant, all residues make an almost equal contribution to its fluctuation. However, in the D76Y mutant, a higher fluctuation was detected at residue 61 to 71, indicating an increase in flexibility in relation to the wild-type. In order to study information over the relative compactness of the protein structure, the radius of gyration was investigated. From the outset of the trajectories to 50 ns, the WT hSOD1 and L67P mutant decreased their Rg values compared to the D76Y mutant, indicating higher protein compactness (**Fig. 4**). Furthermore, to

estimate protein stability, hydrogen bond numbers were analyzed in D76Y and L67P mutants compared to wild-type hSOD1. According to (**Fig. 5**), the average hydrogen bond for wild-type, L67P, and D76Y were 100, 106, and 96, respectively.

#### 5. Discussion

The disease-related mutations and the consequences of these mutations in protein structures have been effectively understood by computer simulations, also known as computer analysis, have effectively understood (25). In this study, the PREDICT SNP integrated server was investigated to predict the possible effects of mutant proteins on enzyme activity. The MAPP and PhD-SNP were algorithms that evaluated the effect of this mutation as destructive. The MAPP algorithm take into consideration the difference in physicochemical properties between mutant residues and wild-type (36). The MAPP uses quantitative scales to measure six physicochemical properties: polarity, hydrophathy, volume free energy, and charge in  $\alpha$ -helix and also  $\beta$ -strand conformations to evaluate missense variants (45). At the same time, PhD-SNP is optimized to predict whether specific protein point mutations can be classified as disease-related polymorphisms (46). Therefore, the results of these two algorithms confirm the association between the destructive effects of the L67P mutation with fALS disease.

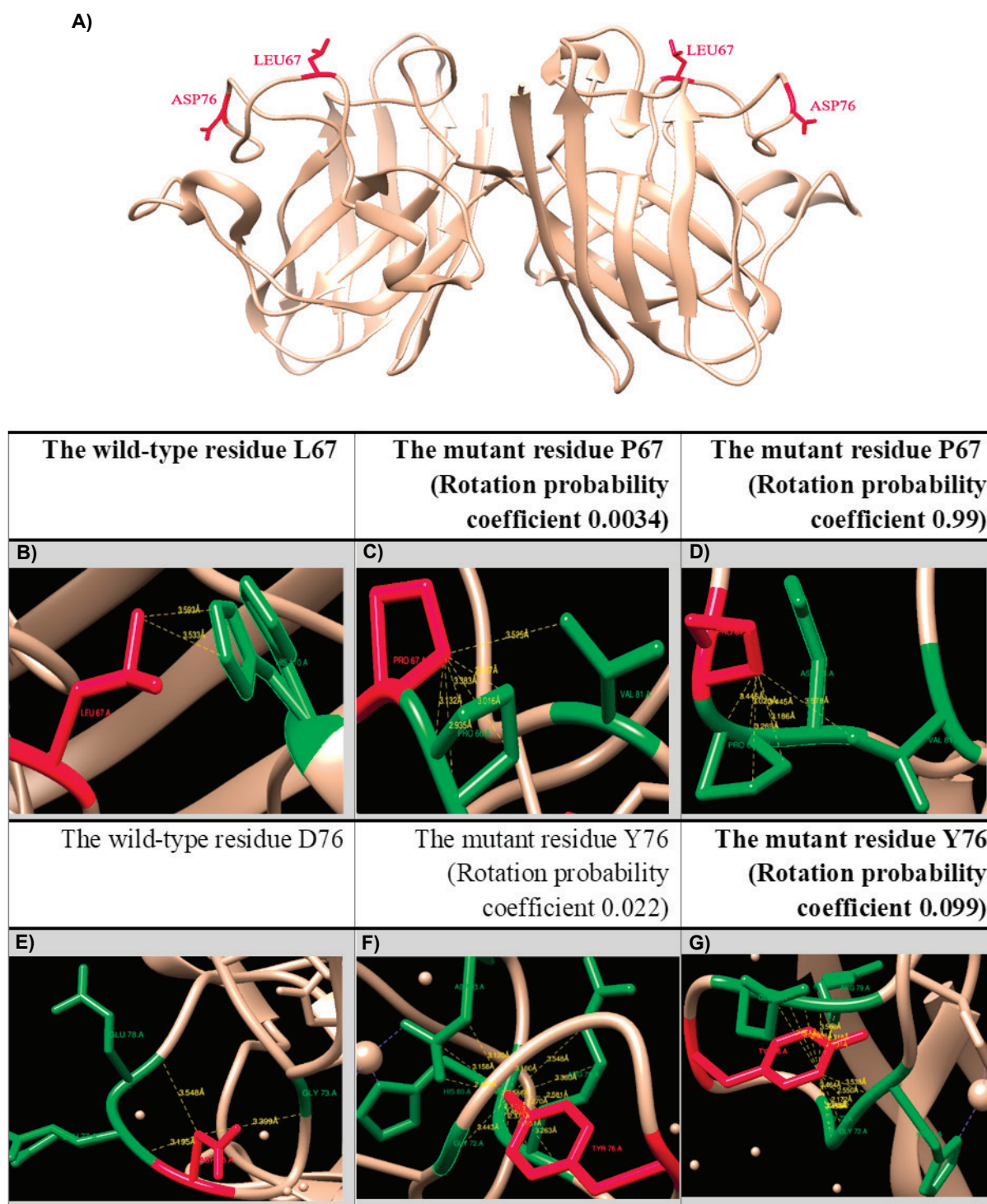


**Figure 1.** A). General schematic of hSOD1 and location of the investigated mutations (L67P and D76Y), (PDB ID: 2C9V). The figure (B-G) was built using the software UCSF Chimera. According analysis in the D76Y variant, the wild-type residue forms a hydrogen bond with: Glycine at position 73 and also the wild-type residue forms a salt bridge with: Arginine at position 79 and Lysine at position 128. The substitution of Asp 76 by Tyr leads to decreased H-bonds. In the L67P variant, the wild-type residue forms a hydrogen bond with: Histidine at position 110. The substitution of Leu 67 by Pro leads to increased hydrophobic bonds with: Arginine at position 69 and Valin 81 and Van Der Waals bond with Asparagine at position 65. For more details, see section results.

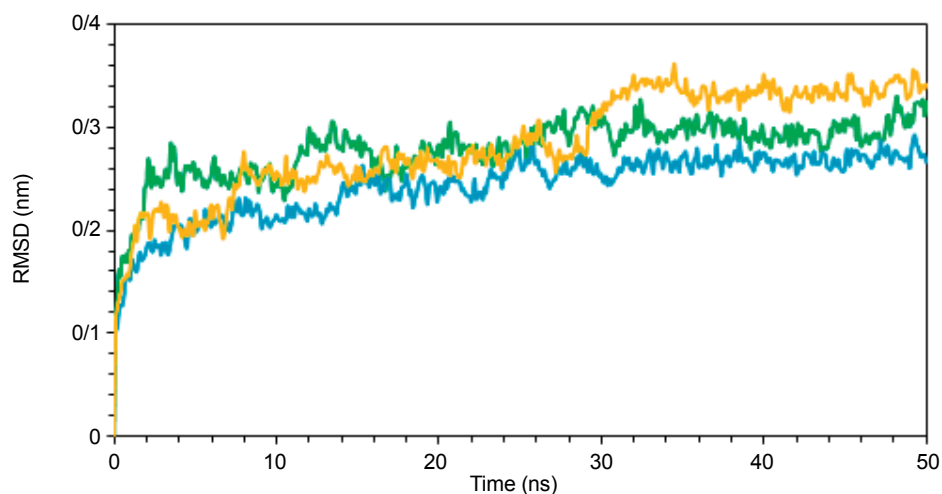


**Figure 2.** RMSD as a function of time. The RMSD for the backbone atoms of the hSOD1 wild-type and the mutants are shown as a function of time. Wild-type is represented in green, the mutant L67P in blue, and the mutant D76Y in yellow. RMSD, root-mean-square deviation; hSOD1, human superoxide dismutase-1.

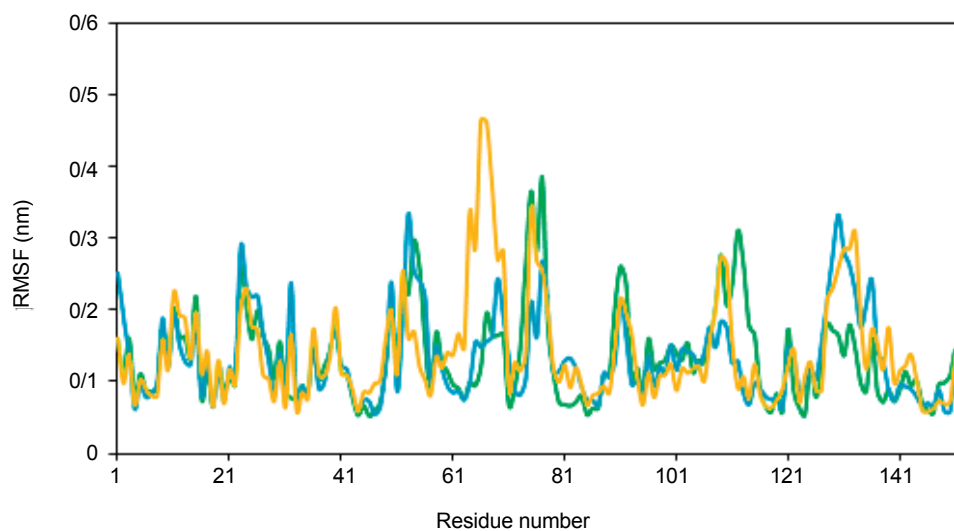


**Figure 3.** RMSF for each residue of hSOD1. Root-mean-square fluctuation for each residue of hSOD1. The wild-type is represented in Green, the L67P variant in blue and the D76Y variant in yellow. RMSF, root-mean-square fluctuation; hSOD1, human Superoxide dismutase-1

These results are consistent with studies by Grande *et al.* (2011) and Krieger *et al.* (2011) on the association of the L67P mutation with ALS disease (13, 15). Also, the results of the D76Y mutation prove to be consistent with what Forsberg *et al.* (2019) provided as findings which confirmed that the D76Y mutation is unstable and destructive (47). Single nucleotide mutations can affect structural stability through changes in free energy

( $\Delta G$  or  $dG$ ). This is if the difference between the free energy change of the wild-type and mutant ( $\Delta\Delta G$  or  $ddG$  (samples is often taken as the coefficient of influence changes in protein stability(48). Some stable 3D conformation of the protein in the folding process in fact corresponds to the minimum level of the Gibbs free energy ( $\Delta G$ ) in the protein-environment system.  $\Delta G$  of folding constitutes both the entropic contributions

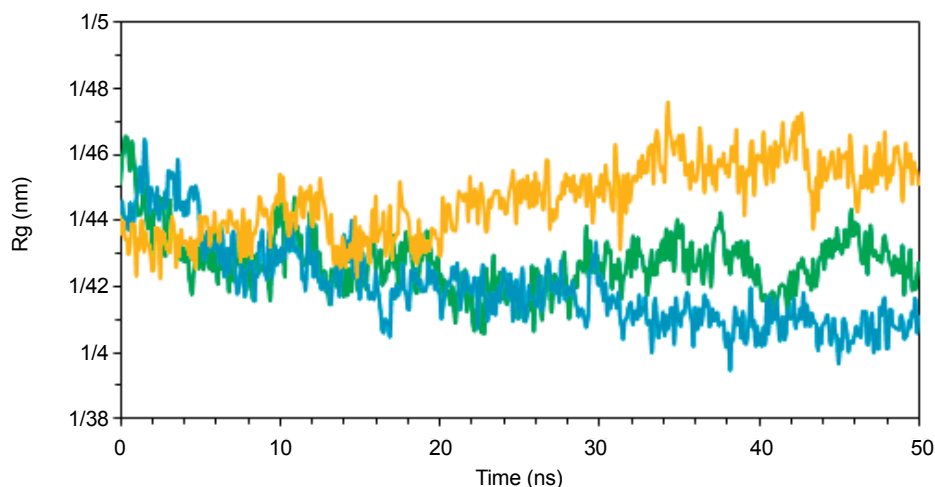


**Figure 4.** Radius of gyration as a function of time. The radius of gyration of the wild-type and the mutants during the MD trajectory is shown. Wild-type is represented in green, the mutant L67P in blue, and the mutant D76Y in yellow. MD, molecular dynamics.

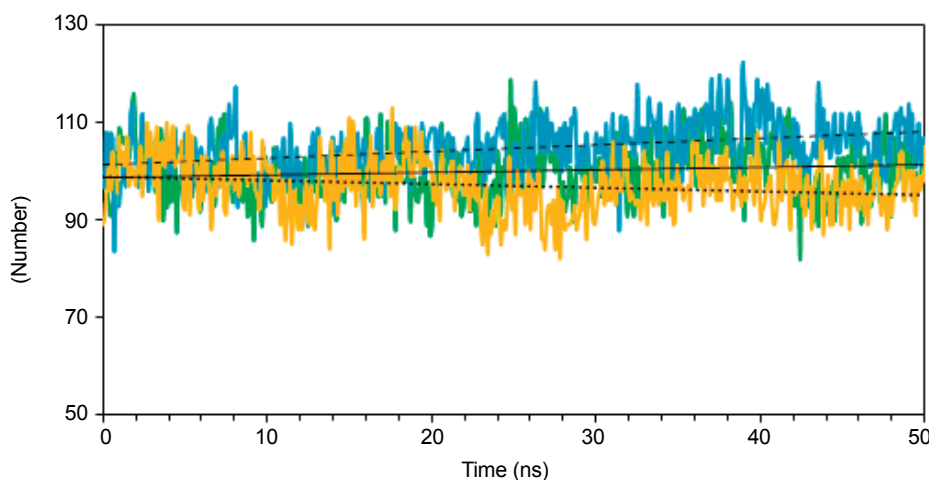


**Figure 5.** Hydrogen bonds (H bond) function of time. The hydrogen bonds of the wild-type and the mutants during the MD trajectory is shown. Wild-type is represented in green, the mutant L67P in blue, and the mutant D76Y in yellow. MD, molecular dynamics. (— Linear Wild-type), (----- Linear L67P), (..... Linear D76Y).

(protein configurations and hydrophobic effect) and the interaction energies in the protein (hydrogen, and electrostatic bonding, hydrophobic interactions etc.) and (49). In fact, the effects exerted by non-synonymous variants on the stability of protein are quantified through using the Gibbs free energy produced by unfolding ( $\Delta G$ ) difference. According to the experimental perspective, the criterion for interest is the difference in

free energy of unfolding between both wild-type and mutated proteins ( $\Delta\Delta G^u$ ). Thus, the equation  $\Delta\Delta G^u = \Delta G^u_{mutant} - \Delta G^u_{wild-type}$  holds, indicating the difference in unfolding free energy between the wild-type and mutated proteins (**Table 2**). The sign  $\Delta\Delta G$  indicates the stability of protein whether the variation decreases ( $\Delta\Delta G^u < 0$ ) or increases ( $\Delta\Delta G^u > 0$ ) the protein stability. Our results exhibit destabilizing effects of L67P and



D76Y mutations on the stability of the WT-hSOD1 structure. This indicates that there is some correlation between the decrease in hSOD1 stability and FALS development. Chimera software was utilized to examine structural changes. This study exhibited that substituting amino acids in the zinc-binding loop causes the removal of previous bonds and the formation of new bonds. Hence, possible rotations of the proline in the L67P mutant and tyrosine in the D76Y mutant caused structural changes. Therefore, these changes may lead to rearrangement of hydrogen bonds and, consequently, changes in enzyme flexibility. Also, changes in bonds due to mutations can affect the proper binding of metals to the appropriate amino acids and, consequently, the correct activity of the enzyme. Moreover, many ALS-related mutations have been shown to be readily misfolded and facilitate interactions in terms of binding both with themselves as well as some other molecules so as to form some aggregates (50-52). In WT hSOD1, leucine 67 contacts with histidine 110 as the distance between the atoms is 3.56 Å (**Fig. 1B**). However, substituting leucine to proline in this position (L67P) causes two rotation probability coefficients. In the first rotation, with rotation probability coefficient 0.0034, proline residue contacts with Val 81 and pro 66 at a distance of 3.7 Å (**Fig. 1C**). In the second rotation, with rotation probability coefficient 0.99, proline contacts with Asn 65, Pro 66, and Val 81 (**Fig. 1D**). The structure of the D76Y mutant is presented in **Figure 1 E-G**, using the software UCSF Chimera, where atoms are numbered following the UCSF Chimera numbering system. In WT hSOD1, the Asp 76 contacts Glu 77, 78, and Gly 73, and the mean distance between the atoms is 3.37 Å (**Fig. 1E**). However, substituting Asp to Tyr in this position (D76Y) causes two rotation probability coefficients. In the first rotation, with rotation probability coefficient 0.022, Tyr 76 contacts with His 80, Arg 79, Asp 83, and Gly 72 (**Fig. 1F**). In the second rotation, with rotation probability coefficient 0.099, Tyr 76 contacts with His 71, Arg 72, Glu 78, and Gly 72,73 (**Fig. 1G**). Molecular dynamics is one of the physical branches of computing. In this method, the interactions between atoms and molecules at intervals of time are simulated by a computer, where the location and velocities of each atom are accurately calculated over time (53). This study was designed to evaluate protein's structural characterization and the conformational preferences of fALS-linked hSOD1 Mutations and

wild-type (L67P and D76Y) using fALS-linked hSOD1 Mutations and simulations of molecular dynamics. In fact, the previous report showed the replacement of leucine by proline at position 67 (L67P) located in the exon 3 hSOD1 gene is associated with the predominant symptoms of lower motor neurons and incomplete penetration (13). Some mutations, like D76Y and G127X, in VII hSOD1 and longer loops IV and, could change their flexibility and also affect the conformation observed in the metal-binding residues (54). However, to further investigate, we carried out an analysis of the influence exerted by two mutations, L67P and D76Y, on the structural stability and molecular dynamics of the hSOD1 through applying some parameters like Rg, RMSF, Rg, hydrogen bonds and RMSD. The RMSD is used to evaluate the stability of the protein structure and characterize the degree of protein structure change (55). In fact, we use RMSD as a helpful parameter to evaluate when the protein converges to achieve some stable position and exhibits the structure stability between mutant hSOD1 and wild-type (9, 40). The results also showed that compared to the wild-type, the D76Y mutant shows some higher (RMSD) than the L67P mutant. The average RMSD of wild-type, L67P, and D76Y were  $0.29 \pm 0.011$  nm,  $0.26 \pm 0.0081$  nm, and  $0.34 \pm 0.0084$  nm, respectively (**Fig. 2**), indicating alteration of the enzyme backbone to some extent. The smaller the numerical value of the RMSD, the more stable the simulated system. Thus, it can be said that the L67P variant had a more stable conformation than D76Y and wild type, which indicates the role of substituted amino acids in reducing structural fluctuations in this mutant compared to D76Y and wild type. In other words, the RMSD values of the D76Y mutant is higher than L67P mutant for all of the period of simulation, suggesting that folding compactness is has improved in L67P mutant in relation to D76Y mutant. These results are consistent with the report of Srinivasan and Rajasekaran (2017) on the structural change of hSOD1 protein due to point mutations (40). In fact, RMSF is measured while considered to be a root mean-square-average distance between an atom or some atoms and the average position it takes in any given structure and it is also defined concerning the displacement of a particular atom or group of atoms (56). We calculated root mean squared fluctuation (RMSF) in order to analyze 153 residues flexibility that are in the structure of mutants and wild type (**Fig. 3**).

Higher RMSF values are often seen in the loops and smaller values in  $\alpha$ -helices (57). Another significant parameter for measuring the compactness of the protein is the radius of gyration (Rg) that usually defined in fact as the mass-weighted root mean square distance of a certain group of atoms from their shared center of mass (5, 24). The average values of Rg for wild-type, L67P, and D76Y were  $1.42 \pm 0.009$ ,  $1.40 \pm 0.012$ ,  $1.45 \pm 0.01$  Å, respectively (**Fig. 4**). since the difference observed in Rg is just  $\sim 0.2$  Å, the smaller deviation observed over the simulation for L67P mutant compared to wild-type is negligible (**Fig. 4**). We also observed a steady behavior in the Rg values from the beginning of the trajectories in the D76Y mutant followed by a sudden Rg value, suggesting replacing aspartic acid with tyrosine at position 76 (D76Y) could affect the protein compactness. Therefore, analysis of Rg exhibited lower compactness in the D76Y mutant and some higher compactness in L67P mutant (**Fig. 4**), suggesting that replacing amino acid at these positions is able to make change in protein compactness relative to the WT protein. We calculated the H-bond number for both mutations to further scrutinize the influence of mutation on the hSOD1 compactness (**Fig. 5**). According to the results H-bond, the L67P mutation increased the number of hydrogen bonds in relation to the wild-type, suggesting reduced flexibility and thus increasing stability, which corresponds to our RMSF. On the other hand, a decrease in the number of hydrogen bond D76Y mutant indicates a decrease in instability and increased protein flexibility. The formation of a hydrogen bond is one of the signs of strengthening the bond and stabilizing any chemical structure. As is well known, hydrogen bonds play a significant role in stabilizing protein structure (58,59). The impact of mutations in hSOD1 on its conformational properties related to amyotrophic lateral sclerosis and the role of occupancy of intramolecular hydrogen bonds between residues using molecular dynamics (MD) simulations were reported by Alemasov *et al.* Hence, the protein residual flexibility results were consistent with the results of studies on structural conformation.

## 6. Conclusion

The mutations scrutinized were found to be positioned in some metal-binding loop region that was highly conserved, making the protein to be structurally instable. First, hSOD1 protein function is predicted

by predicting the SNP integrated server and the  $\Delta\Delta G$  value change single point mutations by applying multiple programs. Further, we analyzed the effect exerted by the substitution mutation on hSOD1 by MD simulations. In fact, our simulations established that D76Y mutation could change the protein conformation significantly thereby leading to some early unfolding. Different parameters that are used in our study showed that L67P mutation on metal-binding loop IV of hSOD1 has completely changed the conformation flexibility and stability. Then, the intermolecular hydrogen bonds created in the protein were significantly increased following the mutation thereby increasing protein stability and compactness. Further, Zn binding loop may form intermolecular interactions in hSOD1, leading form intermolecular interactions in hSOD1, which leads to preservation structural and dynamic, affecting mainly the Zn binding loop. It is important to mention that when hSOD1 loses Zn ion, it induces oxidative damage and leads to protein aggregation. Therefore, the parameters we have used in this study showed that the mutation on the Zn binding loop of hSOD1 has fundamentally changed the flexibility and stability of conformation. Eventually, our research findings provided insight into the effect of mutations on the hSOD1 protein, which in turn leads to neurodegeneration disorders in humans. As a result, this study facilitates understanding the theoretical mechanism associated with the D76Y and L67P mutations in hSOD1 and their subsequent effect on FALS.

**Acknowledgements** We would like to thank to Ms. Hosseini for their technical assistance. This work was supported by University of Mazandaran.

## References

1. Bonnevie V, Dimintyanova K, Hedegaard A, Lehnhoff J, Grøndahl L, Moldovan M, *et al.* Shorter axon initial segments do not cause repetitive firing impairments in the adult presymptomatic G127X SOD-1 Amyotrophic Lateral Sclerosis mouse. *Sci Rep.* 2020;**10**(1):1-16. doi:10.1038/s41598-019-57314-w.
2. Huai J, Zhang Z. Structural properties and interaction partners of familial ALS-associated SOD1 mutants. *Front. Neurol.* 2019;**10**:527. doi:10.3389/fneur.2019.00527.
3. van Es MA, Hardiman O, Chio A, Al-Chalabi A, Pasterkamp RJ, Veldink JH, *et al.* Amyotrophic lateral sclerosis. *The Lancet.* 2017;**390**(10107):2084-2098. doi: 10.1016/S0140-6736(17)31287-
4. Muneeswaran G, Kartheeswaran S, Muthukumar K, Dharmaraj CD, Karunakaran C. Comparative structural

- and conformational studies on H43R and W32F mutants of copper–zinc superoxide dismutase by molecular dynamics simulation. *Biophys. chem.* 2014;**185**:70-78. doi:10.1016/j.bpc.2013.11.010.
5. Nejabat M, Naghash P, Dastsooz H, Mohammadi S, Alipour M, Fardaei M. VSX1 and SOD1 Mutation Screening in Patients with Keratoconus in the South of Iran. *J Ophthalmic Vis Res.* 2017;**12**(2):135. doi: 10.4103/jovr.jovr\_97\_16.
  6. Pansarasa O, Bordoni M, Diamanti L, Sproviero D, Gagliardi S, Cereda C. SOD1 in amyotrophic lateral sclerosis: “ambivalent” behavior connected to the disease. *Int J Mol Sci.* 2018;**19**(5):1345. doi:10.3390/ijms19051345.
  7. Trist BG, Hilton JB, Hare DJ, Crouch PJ, Double KL. Superoxide Dismutase 1 in Health and Disease: How a Frontline Antioxidant Becomes Neurotoxic. *Angew Chem Int Ed.* 2021;**60**(17):9215-9246. doi:10.1002/anie.202000451.
  8. Ihara K, Fujiwara N, Yamaguchi Y, Torigoe H, Wakatsuki S, Taniguchi N, *et al.* Structural switching of Cu, Zn-superoxide dismutases at loop VI: insights from the crystal structure of 2-mercaptoethanol-modified enzyme. *Biosci Rep.* 2012;**32**(6):539-548. doi:10.1042/BSR20120029.
  9. Da Silva ANR, Pereira GRC, Moreira LGA, Rocha CF, De Mesquita JF. SOD1 in amyotrophic lateral sclerosis development—in silico analysis and molecular dynamics of A4F and A4V variants. *J Cell Bio.* 2019;**120**(10):17822-17830. doi:10.1002/jcb.29048.
  10. Rakhit R, Chakrabarty A. Structure, folding, and misfolding of Cu, Zn superoxide dismutase in amyotrophic lateral sclerosis. (*BBA*)-*Mol Basis Dis.* 2006;**1762**(11-12):1025-1037. doi:10.1016/j.bbadis.2006.05.004.
  11. Furukawa Y, O'halloran TV. Posttranslational modifications in Cu, Zn-superoxide dismutase and mutations associated with amyotrophic lateral sclerosis. *Antioxid Redox Signal.* 2006;**8**(5-6):847-867. doi:10.1089/ars.2006.8.847.
  12. Wright GS, Antonyuk SV, Hasnain SS. The biophysics of superoxide dismutase-1 and amyotrophic lateral sclerosis. *Q Rev Biophys.* 2019;**52**. doi:10.1017/S003358351900012X.
  13. Del Grande A, Luigetti M, Conte A, Mancuso I, Lattante S, Marangi G, *et al.* A novel L67P SOD1 mutation in an Italian ALS patient. *Amyotrophic Lateral Sclerosis.* 2011;**12**(2):150-152. doi:10.3109/17482968.2011.551939.
  14. Krieger C, Haase S, Scott P. A second ALS patient having an L67P mutation in exon 3 of the Cu/Zn superoxide dismutase gene. *Amyotrophic Lateral Sclerosis.* 2011;**12**(6):466-467. doi:10.3109/17482968.2011.584630.
  15. Eisen A, Mezei MM, Stewart HG, Fabros M, Gibson G, Andersen PM. SOD1 gene mutations in ALS patients from British Columbia, Canada: clinical features, neurophysiology and ethical issues in management. *Amyotrophic lateral sclerosis.* 2008;**9**(2):108-119. doi: 10.1080/17482960801900073.
  16. Bordo D, Djinovic K, Bolognesi M. Conserved patterns in the Cu, Zn superoxide dismutase family. *J Mol Bio.* 1994;**238**(3):366-386. doi:10.1006/jmbi.1994.1298.
  17. Byström R, Andersen PM, Gröbner G, Oliveberg M. SOD1 mutations targeting surface hydrogen bonds promote amyotrophic lateral sclerosis without reducing apo-state stability. *J Bio Chem.* 2010;**285**(25):19544-19552. doi: 10.1074/jbc.M109.086074.
  18. Getzoff ED, Cabelli DE, Fisher CL, Parge HE, Viezzoli MS, Banci L, *et al.* Faster superoxide dismutase mutants designed by enhancing electrostatic guidance. *Nature.* 1992;**358**(6384):347-351. doi: 10.1038/358347a0
  19. Hörnberg A, Logan DT, Marklund SL, Oliveberg M. The coupling between disulphide status, metallation and dimer interface strength in Cu/Zn superoxide dismutase. *J Mol Bio.* 2007;**365**(2):333-342. doi:10.1016/j.jmb.2006.09.048.
  20. Chng, C. P., & Strange, R. W. Lipid-associated aggregate formation of superoxide dismutase-1 is initiated by membrane-targeting loops. *Proteins: Struct Func Bioinform.* 2014;**82**(11):3194-3209. doi:10.1002/prot.24688.
  21. Shin, D. S., DiDonato, M., Barondeau, D. P., Hura, G. L., Hitomi, C., Berglund, J. A., ... & Tainer, J. A. Superoxide dismutase from the eukaryotic thermophile *Alvinella pompejana*: structures, stability, mechanism, and insights into amyotrophic lateral sclerosis. *J Mol bio.* 2009;**385**(5):1534-1555. doi:10.1016/j.jmb.2008.11.031.
  22. Baziyar, P., B. Seyedalipour, and S. Hosseinkhani, Zinc binding loop mutations of hSOD1 promote amyloid fibrils under physiological conditions: Implications for initiation of amyotrophic lateral sclerosis. *Biochimie,* 2022. **199**: p. 170-181. doi.org/10.1016/j.biochi.2022.05.001.
  23. Chattopadhyay M, Valentine JS. Aggregation of copper–zinc superoxide dismutase in familial and sporadic ALS. *Antioxid Redox Signal.* 2009;**11**(7):1603-1614. doi:10.1089/ars.2009.2536.
  24. Sugaya K, Nakano I. Prognostic role of “prion-like propagation” in SOD1-linked familial ALS: an alternative view. *Front Cell Neurosci.* 2014;**8**:359. doi:10.3389/fncel.2014.00359.
  25. Valentine JS, Doucette PA, Zittin Potter S. Copper-zinc superoxide dismutase and amyotrophic lateral sclerosis. *Annu Rev Biochem.* 2005;**74**:563-593. doi:10.1146/annurev.biochem.72.121801.161647.
  26. Pereira G, Da Silva A, Do Nascimento S, De Mesquita J. In silico analysis and molecular dynamics simulation of human superoxide dismutase 3 (SOD3) genetic variants. *J Cell Biochem.* 2019;**120**(3):3583-3598. doi:10.1002/jcb.27636.
  27. Leinartaitė L, Saraboji K, Nordlund A, Logan DT, Oliveberg M. Folding catalysis by transient coordination of Zn<sup>2+</sup> to the Cu ligands of the ALS-associated enzyme Cu/Zn superoxide dismutase 1. *J Am Chem Soc.* 2010;**132**(38):13495-13504. doi:10.1021/ja1057136.
  28. Tompa DR, Kadirvel S. Molecular dynamics of a far positioned SOD1 mutant V14M reveals pathogenic misfolding behavior. *J Biomol Struct.* 2018;**36**(15):4085-4098. doi: 10.1080/07391102.2017.1407675.
  29. Moradi S, Hosseini E, Abdoli M, Khani S, Shahlaei M. Comparative molecular dynamic simulation study on the use of chitosan for temperature stabilization of interferon αII. *Carbohydr Polym.* 2019;**203**:52-59. doi:10.1016/j.carbpol.2018.09.032.
  30. Nedd S, Redler RL, Proctor EA, Dokholyan NV, Alexandrova AN. Cu, Zn-superoxide dismutase without Zn is folded but catalytically inactive. *J Mol Bio.* 2014;**426**(24):4112-4124. doi.org/10.1016/j.jmb.2014.07.016.
  31. Sirangelo I, Iannuzzi C. The role of metal binding in the amyotrophic lateral sclerosis-related aggregation of copper-zinc superoxide dismutase. *Molecules.* 2017;**22**(9):1429. doi:10.3390/molecules22091429.
  32. Krebs BB, De Mesquita JF. Amyotrophic lateral sclerosis

- type 20-In Silico analysis and molecular dynamics simulation of hnRNPA1. *Plos One*. 2016;**11**(7):e0158939 doi:10.1371/journal.pone.0158939.
33. Kumar CV, Swetha RG, Anbarasu A, Ramaiah S. Computational analysis reveals the association of threonine 118 methionine mutation in PMP22 resulting in CMT-1A. *Adv Bioinform*. 2014;**2014**. doi:10.1155/2014/502618.
  34. Consortium U. UniProt: a hub for protein information. *Nucleic Acid Res*. 2015;**43**(D1):D204-D212. doi: 10.1093/nar/gku989.
  35. Kumar V, Rahman S, Choudhry H, Zamzami MA, Jamal MS, Islam A, *et al.* Computing disease-linked SOD1 mutations: deciphering protein stability and patient-phenotype relations. *Sci Rep*. 2017;**7**(1):1-13. doi: 10.1038/s41598-017-04950-9.
  36. Bendl J, Stourac J, Salanda O, Pavelka A, Wieben ED, Zendulka J, *et al.* PredictSNP: robust and accurate consensus classifier for prediction of disease-related mutations. *PLoS Comput Biol*. 2014;**10**(1):e1003440. doi:10.1371/journal.pcbi.1003440.
  37. Karchin R. Next generation tools for the annotation of human SNPs. *Brief. Bioinform*. 2009;**10**(1):35-52. doi:10.1093/bib/bbn047.
  38. Ng PC, Henikoff S. Predicting the effects of amino acid substitutions on protein function. *Annu Rev Genom Hum Genet*. 2006;**7**:61-80. doi:10.1146/annurev.genom.7.080505.115630.
  39. Zou H, Wu L-X, Tan L, Shang F-F, Zhou H-H. Significance of single-nucleotide variants in long intergenic non-protein coding RNAs. *Fron Cell Dev Bio*. 2020;**8**:347. doi:10.3389/fcell.2020.00347.
  40. Srinivasan E, Rajasekaran R. Exploring the cause of aggregation and reduced Zn binding affinity by G85R mutation in SOD1 rendering amyotrophic lateral sclerosis. *Proteins: Struct Funct Genet*. 2017;**85**(7):1276-1286. doi:10.1002/prot.25288.
  41. Yildiz M, Kocak A. Molecular Dynamics Studies of Histo-Blood Group Antigen Blocking Human Immunoglobulin A Antibody and Escape Mechanism in Noroviruses Upon Mutation. *J Comput Biol*. 2019;**26**(9):962-974. doi:10.1089/cmb.2018.0163.
  42. Harrach MF, Drossel B. Structure and dynamics of TIP3P, TIP4P, and TIP5P water near smooth and atomistic walls of different hydroaffinity. *J Chem Phys*. 2014;**140**(17):174501. doi:10.1063/1.4872239.
  43. Hess B, Bekker H, Berendsen HJ, Fraaije JG. LINCS: a linear constraint solver for molecular simulations. *J Comput Biol*. 1997;**18**(12):1463-1472 doi:10.1002/(SICI)1096-987X(199709)18:12<1463::AID-JCC4>3.0.CO;2-H.
  44. Moradi, M., Hosseinkhani, S., Arab, S. S., & Khammari, A. Effects of Linker Flexibility and Conformational Changes of IP3 Receptor on Split Luciferase Complementation Assay. *Iran J Biotechnol*. 2020;**18**(4):e2423] doi: 10.30498/IJB.2020.2423.
  45. Stone EA, Sidow A. Physicochemical constraint violation by missense substitutions mediates impairment of protein function and disease severity. *Genome Res*. 2005;**15**(7):978-986. doi: 10.1101/gr.3804205.
  46. Capriotti E, Fariselli P, Calabrese R, Casadio R. Predicting protein stability changes from sequeces using support vector machines. *Bioinform*. 2005;**21**(suppl\_2):ii54-ii58. doi:10.1093/bioinformatics/bti110.
  47. Forsberg K, Graffmo K, Pakkenberg B, Weber M, Nielsen M, Marklund S, *et al.* Misfolded SOD1 inclusions in patients with mutations in C9orf72 and other ALS/FTD-associated genes. *J Neurol Neurosurg Psychiatry*. 2019;**90**(8):861-869. doi:10.1136/jnnp-2018-319386.
  48. Chen C-W, Lin J, Chu Y-W, editors. iStable: off-the-shelf predictor integration for predicting protein stability changes. *BMC Bioinform*. 2013: *BioMed Central*. doi:10.1186/1471-2105-14-s2-s5.
  49. Steff S, Nishi H, Petukh M, Panchenko AR, Alexov E. Molecular mechanisms of disease-causing missense mutations. *J Mol Bio*. 2013;**425**(21):3919-3936. doi:10.1016/j.jmb.2013.07.014.
  50. Chiti F, Taddei N, Baroni F, Capanni C, Stefani M, Ramponi G, *et al.* Kinetic partitioning of protein folding and aggregation. *Nat Struct Biol*. 2002;**9**(2):137-143. doi:10.1038/nsb752.
  51. Otzen DE, Kristensen O, Oliveberg M. Designed protein tetramer zipped together with a hydrophobic Alzheimer homology: a structural clue to amyloid assembly. *Proc Natl Acad Sci*. 2000;**97**(18):9907-9912. doi:10.1073/pnas.160086297.
  52. Sandelin E, Nordlund A, Andersen PM, Marklund SS, Oliveberg M. Amyotrophic lateral sclerosis-associated copper/zinc superoxide dismutase mutations preferentially reduce the repulsive charge of the proteins. *J Bio Chem*. 2007;**282**(29):21230-21236. doi:10.1074/jbc.M700765200.
  53. Ramanathan A, Agarwal PK, Kurnikova M, Langmead CJ. An online approach for mining collective behaviors from molecular dynamics simulations. *J Comput Bio*. 2010;**17**(3):309-324. doi:10.1089/cmb.2009.0167.
  54. Das A, Plotkin SS. Mechanical probes of SOD1 predict systematic trends in metal and dimer affinity of ALS-associated mutants. *J Mol Bio*. 2013;**425**(5):850-874. doi:10.1016/j.jmb.2012.12.022.
  55. Zhao X, Liu R, Miao Z, Ye N, Lu W. A Study of Potential SARS-CoV-2 Antiviral Drugs and Preliminary Research of Their Molecular Mechanism, Based on Anti-SARS-CoV Drug Screening and Molecular Dynamics Simulation. *J Comput Bio*. 2020. doi:10.1089/cmb.2020.0112.
  56. Martínez L. Automatic identification of mobile and rigid substructures in molecular dynamics simulations and fractional structural fluctuation analysis. *Plos One*. 2015;**10**(3):e0119264. doi:10.1371/journal.pone.0119264.
  57. Mutter ST, Turner M, Deeth RJ, Platts JA. Molecular dynamics simulations of copper binding to amyloid-β Glu22 mutants. *Heliyon*. 2020;**6**(1):e03071. doi:10.1016/j.heliyon.2019.e03071.
  58. Alesanov NA, Ivanisenko NV, Medvedev SP, Zakian SM, Kolchanov NA, Ivanisenko VA. Dynamic properties of SOD1 mutants can predict survival time of patients carrying familial amyotrophic lateral sclerosis. *J Biomol Struct Dyn* 2017;**35**(3):645-656. doi:10.1080/07391102.2016.1158666.
  59. Alesanov NA, Ivanisenko NV, Ramachandran S, Ivanisenko VA. Molecular mechanisms underlying the impact of mutations in SOD1 on its conformational properties associated with amyotrophic lateral sclerosis as revealed with molecular modelling. *BMC Struct. Biol*. 2018;**18**(1):1-14. doi:10.1186/s12900-018-0082-7.